*Translational Animal Science*, 2022, **6**, 1–14
https://doi.org/10.1093/tas/txac066
Advance access publication 18 May 2022
**Technology in Animal Science**

# Estimation of empty body and carcass chemical composition of lactating and growing cattle: comparison of imaging, adipose cellularity, and rib dissection methods

**Caroline Xavier,[†,‡] Charlotte Driesen,[†,‖] Raphael Siegenthaler,[$] Frigga Dohme-Meier,[†] Yannick Le Cozler,[‡] and Sylvain Lerch[†,1]**

[†]Ruminants Research Group, Agroscope, 1725 Posieux, Switzerland
[‡]PEGASE INRAE-Institut Agro Rennes-Angers, 16 Le Clos, 35590 Saint Gilles, France
[‖]Empa, Laboratory for Advanced Analytical Technologies, Überlandstrasse 129, 8600 Dübendorf, Switzerland
[$]Research Contracts Animals Group, Agroscope, 1725 Posieux, Switzerland

[1]Corresponding author: sylvain.lerch@agroscope.admin.ch

## ABSTRACT

The aim of present study was to compare in vivo and post mortem methods for estimating the empty body (EB) and carcass chemical compositions of Simmental lactating and growing cattle. Indirect methods were calibrated against the direct post mortem reference determination of chemical compositions of EB and carcass, determined after grinding and analyzing the water, lipid, protein, mineral masses, and energy content. The indirect methods applied to 12 lactating cows and 10 of their offspring were ultrasound (US), half-carcass and 11th rib dual-energy X-ray absorptiometry (DXA) scans, subcutaneous and perirenal adipose cell size (ACS), and dissection of the 11th rib. Additionally, three-dimensional (3D) images were captured for 8 cows. Multiple linear regressions with leave-one-out-cross-validations were tested between predictive variables derived from the methods tested, and the EB and carcass chemical compositions. Partial least square regressions were used to estimate body composition with morphological traits measured on 3D images. Body weight (BW) alone estimated the EB and carcass composition masses with a root mean squared error of prediction (RMSEP) for the EB from 1 kg for minerals to 12.4 kg for lipids, and for carcass from 0.9 kg for minerals to 7.8 kg for water. Subcutaneous adipose tissue thickness measured by US was the most accurate in vivo predictor when associated with BW to estimate chemical composition, with the EB lipid mass RMSEP = 11 kg and $R^2$ = 0.75; carcass water mass RMSEP = 6 kg and $R^2$ = 0.98; and carcass energy content RMSEP = 236 MJ and $R^2$ = 0.91. Post mortem, carcass lipid mass was best estimated by half-carcass DXA scan (RMSEP = 2 kg, $R^2$ = 0.98), 11th rib DXA scan (RMSEP = 3 kg, $R^2$ = 0.96), 11th rib dissection (RMSEP = 4 kg, $R^2$ = 0.92), and perirenal ACS (RMSEP = 6 kg, $R^2$ = 0.79) in this respective order. The results obtained by 11th rib DXA scan were accurate and close to the half-carcass DXA scan with a reduction in scan time. Morphological traits from 3D images delivered promising estimations of the cow EB and carcass chemical component masses with an error less than 13 kg for the EB lipid mass and than 740 MJ for the EB energy. Future research is required to test the 3D imaging method on a larger number of animals to confirm and quantify its interest in estimating body composition in living animals.

**Key words:** body composition, dual-energy X-ray absorptiometry, ruminant, three-dimensional imaging, ultrasound

## INTRODUCTION

In vivo estimation of livestock body composition is mandatory to access the dynamics of mobilization and accretion of body reserves along the production cycle. Such an estimation is also of interest to determine the commercial value of the carcass. Methods to estimate the body and carcass composition are diverse (Lunt et al., 1985; Scholz et al., 2015; Lerch et al., 2021). Most evaluations performed on-farm are based on human expertise and are completed via carcass information after slaughter. Direct estimations on living animals are also possible thanks to noninvasive and nondestructive methods, such as image-based techniques like ultrasound (US), two-dimensional (2D) or three-dimensional (3D) X-ray imaging, as well as 3D imaging based on 3D cameras. Ultrasound is used to monitor body lipid dynamics in dairy cows (Waltner et al., 1994; Schröder and Staufenbiel, 2006) and carcass traits in beef cattle (Greiner et al., 2003; Bergen et al., 2005) at a relatively low cost; however, its accuracy depends on the animal model studied (Lerch et al., 2021). Alternatively, computed tomography (CT), dual-energy X-ray absorptiometry (DXA), and magnetic resonance imaging (MRI), provide fine quantification of whole body or carcass compositions, and are therefore more accurate than US (Scholz et al., 2015). Nonetheless, due to the cost of devices, safety issues regarding exposure to X-ray (CT scan and to a lesser extent, DXA), or the time needed for a full body scan and postacquisition treatment, these technologies are not easy to use at a large scale. In addition, they cannot be used on larger living animals, such as cow or beef, due to their size in comparison to the device capacity (e.g., bovine has a BW higher than 200 kg), whereas for smaller animals, such as sheep or goat, the need of no movement results in a routine use of anesthesia (Hunter et al., 2011). Still, the use of DXA, in order to estimate the carcass tissue composition in beef cattle, was previously explored (Lopez-Campos et al., 2018; Calnan et al., 2021; Segura et al., 2021). Recently, interest in the imaging of living beef cattle

Received May 9, 2022 Accepted May 18, 2022.

also increased with the development of in vivo 3D imaging thanks to 3D cameras (Gomes et al., 2016; Miller et al., 2019; Cominotte et al., 2020).

To be fully recognized as an accurate method of interest, imaging techniques need to be compared with the established reference method (i.e., "gold standard"), that is for chemical composition, the chemical analysis of homogenate of the EB or carcass after post mortem grinding. Their results need also to be compared to those from other well-established methods, like the dissection of a single (Geay and Béranger, 1969; Robelin and Geay, 1976; Fiems et al., 2005) or multiple rib cut (Hankins and Howe, 1946; Mitchell et al., 1997, Ribeiro et al., 2011; Berndt et al., 2017), which are often used to estimate the composition of the whole carcass. Another classical method to estimate the EB composition is the measurement of adipose cell size (ACS; Hood and Allen, 1973, Waltner et al., 1994). In a recent methodological paper (Lerch et al., 2021), several of these in vivo methods were compared to the reference post mortem chemical analysis method in dairy goats.

The aim of the present study was to calibrate and compare several methods to determine the body composition of large animals, such as lactating cows and growing cattle. The results from the imaging technics, i.e., in vivo US of the back fat thickness, 3D scan of the full body, post mortem DXA scan of the half-carcass or 11th rib cut, and ACS measurements and 11th rib cut dissection, were all compared to the reference chemical compositions of EB and carcass. Lactating cows and growing cattle were studied together to represent the diversity of animal types present in bovine farms, considering the interest for future routine use. Indeed, in bovine farms, dairy, or suckling cows are often present simultaneously with growing and fattening beef cattle and/or renewal heifers.

## MATERIALS AND METHODS

### Animals

All procedures performed on animals were approved by the ethics committee of the Fribourg cantonal state (n°2018_08_FR). The study was performed at the experimental farm of Agroscope Posieux (Switzerland) and involved 12 Simmental lactating cows (six primiparous and six multiparous) weighing 519 to 664 kg, and 10 of their offspring (seven heifers and three castrated males) weighing 290 to 403 kg. Cows came from 9 different commercial farms.

Cows were fed ad libitum (10% refusals) daily at 14:00 h with grass silage and milked twice per day (06:00 h and 16:00 h). Calves were fed with milk of their respective dams, and received additionally concentrate and ad libitum hay. Full details about feeding and housing conditions are described in Driesen et al. (2022).

### Direct Post-slaughter Measurements of Empty Body and Carcass Chemical Compositions

Animals were slaughtered at 288 ± 4.5 days in milk (cow) or days old (calves) at the experimental slaughterhouse of Agroscope Posieux by stunning with captive bolt followed by exsanguination, in accordance with legally defined procedures. Animals were weighed before and after exsanguination, and blood samples were collected during exsanguination. One aliquot of blood (250 g) served for dry matter (DM) content determination, whereas a second aliquot of blood (600 g) was centrifuged (relative centrifugal force = 3000 *g*, 15 min, at ambient temperature) before blood serum and blood cell sampling, followed by storage at –20 °C, pending chemical analyses. The head, tail, lower legs, hide, and viscera (internal organs and full digestive tract) were removed according to classical commercial procedures, and every part was weighed separately. The bladder was weighed full and empty. The full digestive tract was further separated into reticulo-rumen, omasum, abomasum, intestines, and omental and mesenteric adipose tissues (AT). Digestive tract sections were further emptied and weighed individually, in order to compute, by difference, the weight of digesta. Empty BW was defined as *pre*-slaughter BW *minus* the weight of digesta and urine. Blood weight was computed as the exsanguinated blood (difference between *pre*- and *post*-exsanguination weights) plus the difference between empty BW and the sum of every non-blood EB compartment weighed separately.

The carcass was split along the spinal column into two equal parts, which were individually weighed (hot half-carcass weights). Both half-carcasses were chilled at 4 °C for 24 h before weighing (cold weights). As chemical composition of both half-carcasses was considered equal, only measurements and chemical analysis were performed on the left half-carcass. The cold left half-carcass and the rest of the EB (without blood) were stored at –20 °C and later, grinded separately using an industrial crusher (Granulator type PS 4-5, Pallmann Industries, Pompton Plains, USA) to render small blocks mixed homogeneously (Mixer type MIX 165, Talsa, Spain). They were then grounded again using a cutter device (Cutter DMK 45 C, DMS-Maschinensysteme, Saarbrücken, Germany). After these two grinding steps and thoroughly homogenization, one sample (1 kg) of grinded half-carcass, and one of the rest of the EB were sampled and frozen (–20 °C), before being finely minced (Mincer type TWK 98, Kolbe foodtech, Elchingen, Germany). Two 250 g aliquots were ultimately sampled and frozen (–20 °C) pending chemical analyses.

The DM of the full blood collected at exsanguination was determined by oven desiccation (60 °C for 72 h). The proportions of mineral, lipid, and protein in full blood DM were computed from hematocrit values (Vetscan HM5, Abaxis, Griesheim, Germany), serum lipid (liquid–liquid extraction, Driesen et al., 2022), and protein (BT1500 autoanalyzer, Biotecnica Instruments, Roma, Italy) contents, and blood cells composition. Frozen homogenous samples of the blood cell, half-carcass, and the rest of the EB were lyophilized and finely ground with liquid nitrogen using a knife mill (Grindomix GM200, Retsch, Haan, Germany). Laboratory DM (3 h at 104 °C), mineral (oven at 550 °C until constant weight), lipid (ISO 6492:1999, petroleum ether extraction with a Büchi Speed Extractor E-916, Flawil, Switzerland), protein (ISO 16634-1:2008, N x 6.25 by Dumas combustion – thermal conductivity with a Leco Trumac CNS, St. Joseph, Michigan, USA), and energy (ISO 9831:1998, adiabatic calorimetry with an oxygen bomb calorimeter, AC600 LECO, Mönchengladbach, Germany) contents were further determined.

Chemical composition in proportions of the hot right half-carcass was assumed equal to the one of the left side. The left-carcass proportions were applied at the right-side hot carcass weight to obtain the whole hot carcass composition in masses. Chemical composition of the EB was defined as the sum of the chemical composition reconstituted for the whole hot carcass, the chemical composition of the rest of the EB, and

the chemical composition of the blood. Constant weighing and reweighing procedures before and after the freezing steps were ensured, and any weight loss from the initial weighing at the slaughterhouse was assumed to be water loss.

## Methods Tested for Estimating Empty Body and Carcass Chemical Compositions

**In vivo methods.** The day before slaughter, an US image was recorded on the left side of each animal, located at one-third of the ischium–sacrum distance (Realini et al., 2001; Schröder and Staufenbiel, 2006). A Logiq e R7 US machine equipped with a 9L-RS Linear-Transducer (3.0–9.0 MHz; GE Healthcare, Glattbrugg, Switzerland) was used. The thickness of the subcutaneous adipose tissue was further estimated as the average thickness measurement between the maximum and minimum thickness of the tissue recorded on the image without the skin (Realini et al., 2001), which was analyzed using the ImageJ software (1.52r version, National Institute of Health, USA). The thickness of muscle was not treated because of the difficulties to locate precisely the lower muscle fascia for 11 images on 22. The day before slaughter, the body shape of 8 cows was recorded using a 3D imaging device (Morpho3D), similar to the one presented by Le Cozler et al. (2019a). Briefly, this device is composed of five cameras paired with infrared lasers installed on a sliding mobile portal that scans the animal from tail to head. The images were processed as described by Le Cozler et al. (2019a) after a single operator performed the following linear measurements: wither height, hip height, back length between wither and sacrum, hip width, chest depth, and the diagonal length between the shoulder and the opposite ischium. Heart girth, partial volume, and partial surface were also determined (as previously defined by Le Cozler et al., 2019b; Figure 1).

Following recommendations from Robelin (1981), immediately after slaughter, subcutaneous AT located at one-third of the ischium–sacrum distance (similar localization than for US measurement) and perirenal AT were sampled. Around 0.5 g were maintained in a physiological saline solution at 39 °C. Adipose samples were then cut in small cubes, washed with saline solution, and fixed in a 4% osmium tetroxide solution within 2 h following sampling. One week later, ATs were mechanically disaggregated and washed with distilled water. Adipose cells were trapped by filtration on a 0.45 µm-pore filter (Robelin, 1981) before being resuspended in a 0.01% Triton X100 solution and measured on a BX53 microscope (Olympus Schweiz AG, Wallisellen, Switzerland). The diameter of at least 200 adipose cells was determined using ImageJ software.

**Post mortem methods.** The day after slaughter, the 10th to 12th rib section was removed from the left half-carcass. The limit of the section was defined by a line parallel to the spine axis passing through the point of the ilium at the 11th rib and reaching straightly the 5th intercostal space (6 and 7 ribs intercostal space). The left 11th rib cut was further precisely separated from the 10–12 rib section at exact intercostal mid-distances between 10th to 11th and 11th to 12th ribs (Geay and Béranger, 1969).

A DXA scanner GE Lunar (iDXA Model, General Electrics Medical Systems, Glattbrugg, Switzerland) was used to scan the left cold half-carcass and the left 11th rib before dissection. The DXA scanner used pencil beam technology with X-ray spectra at two different photon energy levels. Before each scan series, the reliability of the internal calibration was assessed using a phantom (calibration object) and following the manufacturer's instructions. The left half-carcass was scanned using the human total body mode (100 kV, 0.188 mA) and the 11th rib using the small animal body mode (100 kV, 0.188 mA). Lean, fat, and bone mineral content (BMC) mass variables were selected after image post processing treatment in "Right Arm" mode, according to Hunter et al. (2011). Artefacts were checked individually and the correct assignation to the corresponding tissue was verified. Two (for calves) or three (for cows) successive scans were required for performing the full scan of the half-carcass previously cut into five parts (Supplementary Figure S1), since the DXA scanner table was not large and long enough. The results of the 2–3 scans were further summed in order to compute the

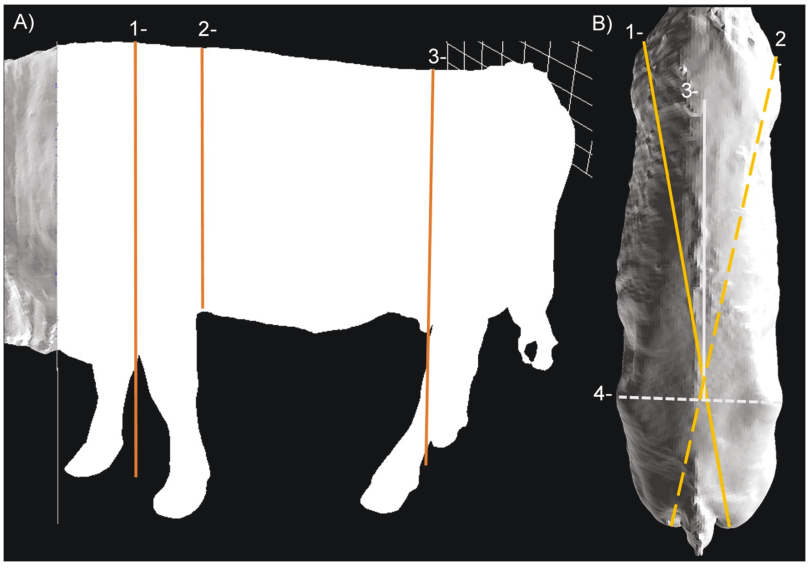


**Figure 1.** Measurements on 3D image of a Simmental cow: A) White area represents partial volume and surface, 1: wither height, 2: chest depth and hearth girth, 3: hip height, B) 1 and 2: diagonal lengths, 3: back length, and 4: hip width.

total half-carcass values. Immediately after its DXA scan, the 11th rib was weighed, before being dissected anatomically by a single professional butcher operator, in order to further weigh separately the lean, AT (subcutaneous and intermuscular), and bone.

### Statistical Analyses

All statistics were performed with R software (version 3.6.3, R Core Team, 2020). Simple and multiple linear regressions were performed with the "lm" function (R package "stats", R Core Team, 2020) to estimate body and carcass reference chemical composition from the US, DXA, ACS, or 11th rib cut dissection variables. For the EB chemical composition, only subcutaneous ACS and US were tested, as these were the only methods accessible in vivo. For all these estimations, the effect of animal type (cow or calf) was tested on intercept and slope.

The backward selection process was applied to define variables of interest and significant ($P < 0.05$) or tendency ($0.05 < P < 0.10$) variables were selected. This selection was realized based on type 3 ANOVA (R package "car"; Fox and Weisberg, 2019). Equations with better estimations than those with BW or carcass weight alone were calibrated and validated based on the main dataset with a leave-one-out-cross-validation, which was performed with the R package "caret" (Kuhn, 2021). The results include the determination coefficient ($R^2$) and the root mean square error of prediction (RMSEP).

Data from 3D imaging analyses ($n = 8$ cows) were treated by partial least square (PLS) regression with a leave-one-out-cross-validation method (R package "pls"; Mevik et al., 2020) in order to analyze the relationship between in vivo body measurements, EB, carcass chemical composition, and 3D variables. The PLS regression allows to take into account the strong correlation between predictive variables (Supplementary Table S1) and the large number of predictive variables ($n = 10$, when having access to a limited number of observations: i.e., 8 cows). The predictive 3D variables were standardized thanks to the "Scale" option of the function "plsr", and were integrated in Latent variables to explain the outcome variable. The presented RMSEP corresponded to the adjusted RMSEP calculated by the package "pls," and the $R^2$ is the variance explained by the model. Models were compared with each other based on the value of $R^2$, RMSEP, and the residual coefficient of variation (rCV; ratio of RMSEP to the mean of the dependent variable).

## RESULTS

### Post mortem Chemical Composition and Anatomical Measurements

The body, carcass weights, and chemical compositions are reported in Table 1. The body weight before slaughter averaged 483 kg, ranging from 291 (calf) to 663 (cow) kg. Hot carcasses weighed on average 244 kg ranging from 139 to 331 kg. On average, both cows and calves EB and carcass were composed of 61% ± 3% (mean ± SD) water, and 18% (±1%) proteins. Calves had a lipid content of 10% to 25% in EB and 10% to 24% in carcass, conversely to cows, which had a narrower range of 13% to 22% and 12% to 21%, respectively. Mineral content was 4% (±0.3%) in EB and 5% (±0.4%) in carcass.

Empty body lipid and water proportions were highly negatively correlated ($r = -0.98$, $P < 0.05$, Figure 2). The percentage of water in fat-free EB (EB total mass – EB lipid mass) was almost constant between 73% and 76%, as well as proteins (20–23%) and minerals (4–5%).

**Table 1.** Anatomical and chemical component masses of empty body and carcass measured after slaughter of 6 primiparous and 6 multiparous Simmental cows ($n = 12$) and calves ($n = 10$) at 288 days in milk or old, respectively

| | All | | | | Cows | | | | Calves | | | |
|---|---|---|---|---|---|---|---|---|---|---|---|---|
| | Mean | SD | Min | Max | Mean | SD | Min | Max | Mean | SD | Min | Max |
| Preslaughter body weight, kg | 483 | 126 | 291 | 663 | 589 | 46 | 519 | 663 | 355 | 33 | 291 | 403 |
| Digesta, kg | 73 | 23 | 38 | 112 | 91 | 10 | 75 | 112 | 50 | 9 | 38 | 67 |
| Empty body weight (without urine and digesta; kg) | 409 | 104 | 238 | 564 | 497 | 40 | 435 | 564 | 304 | 32 | 238 | 336 |
| Hot carcass weight, kg | 244 | 66 | 139 | 331 | 300 | 24 | 267 | 331 | 178 | 20 | 139 | 204 |
| Cold carcass weight (24 h at 4°C; kg) | 240 | 65 | 136 | 325 | 295 | 24 | 263 | 325 | 175 | 20 | 136 | 200 |
| Carcass yield (hot carcass weight/body weight; %) | 50.5 | 1.4 | 48.0 | 52.9 | 50.9 | 1.1 | 48.8 | 52.5 | 50.0 | 1.6 | 48.0 | 52.9 |
| Empty body, kg | | | | | | | | | | | | |
| Water | 249.4 | 64.7 | 158.1 | 337.3 | 304.8 | 19.1 | 280.4 | 337.3 | 182.8 | 17.6 | 158.1 | 210.7 |
| Lipid | 72.5 | 22.7 | 24.2 | 122.2 | 85.9 | 19.7 | 57.6 | 122.2 | 56.5 | 14.2 | 24.2 | 79.6 |
| Protein | 71.6 | 17.4 | 44.3 | 96.1 | 86.4 | 5.9 | 75.6 | 96.1 | 53.9 | 5.4 | 44.3 | 61.5 |
| Mineral | 16.0 | 4.5 | 8.4 | 21.6 | 19.8 | 1.3 | 16.9 | 21.6 | 11.4 | 1.2 | 8.4 | 12.3 |
| Energy, MJ | 4,464 | 1,242 | 1,922 | 7,004 | 5,345 | 872 | 4,061 | 7,004 | 3,407 | 629 | 1,922 | 4,343 |
| Hot carcass, kg | | | | | | | | | | | | |
| Water | 148.9 | 39.5 | 93.9 | 206.9 | 182.4 | 13.0 | 165.7 | 206.9 | 108.7 | 11.8 | 93.9 | 129.2 |
| Lipid | 41.1 | 14.2 | 13.5 | 69.9 | 50.6 | 10.8 | 32.4 | 69.9 | 29.7 | 7.8 | 13.5 | 45.3 |
| Protein | 42.6 | 11.2 | 25.9 | 58.2 | 52.0 | 4.2 | 44.2 | 58.2 | 31.3 | 3.4 | 25.9 | 36.7 |
| Mineral | 11.4 | 3.4 | 5.5 | 15.9 | 14.2 | 1.1 | 12.0 | 15.9 | 7.9 | 1.0 | 5.5 | 8.7 |
| Energy, MJ | 2,597 | 794 | 1,127 | 4,059 | 3,200 | 479 | 2,501 | 4,059 | 1,872 | 347 | 1,127 | 2,490 |

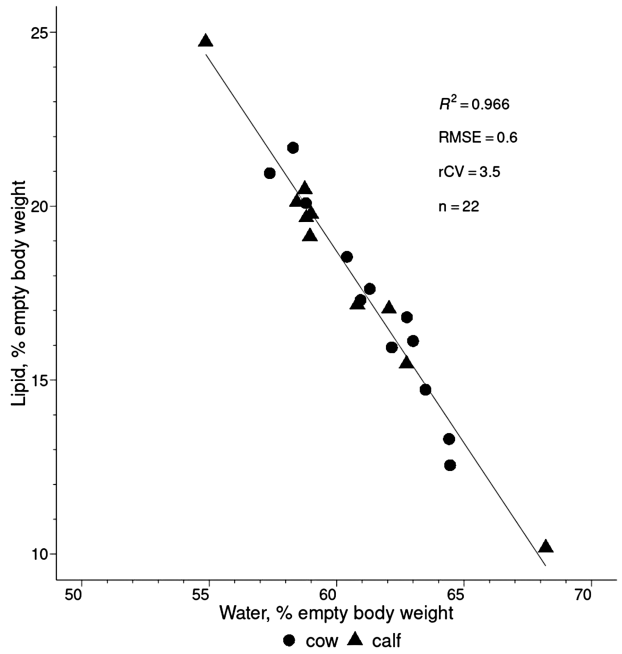


**Figure 2.** Relationship between water and lipid contents of Simmental cows ($n$ = 12) and calves ($n$ = 10) on an empty body basis.

## Variables Derived from the Methods Tested

The different measurements from the tested methods are presented in Table 2. Subcutaneous AT thickness measured by US averaged 0.69 cm. A coefficient of variation of 53.9% was recorded in cows, whereas this variation was 40.9% for calves. On average, the 11th rib cut weighed 1,016 g (248 g to 1,397 g, Table 2), with an obvious difference between calves and cows. The muscles formed the majority of the rib with 610 g, followed by AT with 231 g, and bones with 195 g. The coefficient of variation of the muscles in cows was 10% and 15% in calves. For AT, it was 25% for cows and 26% for calves. The variation in bones was 12% for both groups. Cold half-carcass total mass acquired by DXA was 122 kg, with DXA lean mass content of 98 kg, ranging from 61 kg to 134 kg (Table 2). Variations were more important for DXA fat mass, ranging from 6 kg to 30 kg with a mean value of 18 kg, and for DXA BMC mass, ranging from 3 kg to 9 kg with a mean value of 6 kg. Variations were more important for calves, with the highest variation for DXA fat mass (26%). Variations were 3% lower for cow measurements, except for DXA BMC mass, where a difference of 2% was noticed. The total mass of the 11th rib estimated by DXA was 1,191 g (1,029 g to 1,374 g) for cows and 817 g (660 g to 918 g) for calves. For the 11th rib of all animals, the DXA estimated lean mass was 676 (±150) g, fat mass was 289 (±83) g, and BMC mass was 55 (±18) g. Calves presented more variations between the different masses of tissue, except for DXA fat mass. Adipose cell size was higher for the perirenal AT depot (144 ± 18 µm) compared to the subcutaneous one (123 ± 14 µm). Additionally, variability recorded in subcutaneous and perirenal ACS was around 12% for cows and calves.

Table 3 presents all the body measurements for the 8 cows, as determined from 3D imaging. The wither and hip heights were very close, with around 142 cm and a coefficient variation of only 2%. The other measurements were the hip width (55 ± 3 cm), chest depth (79 ± 3 cm), and heart girth (210 ± 5 cm). For all these measurements, coefficient of variation was reduced and ranged from 2% to 5%. The length of the back between the wither and the hip point was 87 cm, and the diagonal length averaged 163 cm, ranging from 150 cm to 180 cm. Partial volume (volume without the head and neck anterior to the shoulder line volumes) presented the largest variation, with a coefficient of variation of 9% (598 ± 56 L), ranging from 529 L to 655 L. The partial surface was 5.2 ± 0.3 m$^2$ (4.8 m$^2$ to 5.6 m$^2$, 6% coefficient of variation).

## Estimation of Empty Body Chemical Component Masses

The relationships for the estimation of the EB chemical component masses are presented in Table 4 and Figure 3. Combining cow and calf data, BW alone explained 0.976 of the variance of the EB water mass, 0.936 of the variance of the EB mineral mass, and 0.973 of the variance of the EB protein. The rCV was 4% for the EB protein and water masses, and it was 7% for the EB mineral mass. None of the variables derived from the in vivo methods tested (e.g., US) improved the $R^2$ and RMSEP of the protein and mineral EB masses when compared to the $R^2$ and RMSEP obtained with relationships with BW alone. Conversely, the addition of the subcutaneous ACS or US AT thickness to the BW improved the relationship for the estimation of water mass (rCV decreased by –0.3% to –0.4%). The explanation of the variance by BW was less important for the EB energy content, with $R^2$ = 0.840, and for the EB lipid mass, $R^2$ = 0.688.

Of all the in vivo methods tested to estimate the EB chemical masses, the thickness of the subcutaneous AT measured by US associated with BW provided the best relationship, with a decrease of the rCV of –1.7% for lipid mass and –0.9% for energy content. Adding the subcutaneous ACS to the BW improved the relationship with a decrease of the rCV of –1.5% for lipid mass and –0.8% for the EB energy content when compared to BW alone.

## Estimation of Carcass Chemical Component Masses

The relationships for the estimation of carcass chemical component masses are presented in Table 5 and Figure 4. Body weight or carcass weight alone explained more than 0.74 of the lipid carcass mass and more than 0.89 of the other components, including energy. For these relationships, the maximum rCV was 17% for lipid mass, 10% for energy, 8% for mineral mass, 5% for protein mass, and 5% for water mass. The BW alone estimated lipid mass, mineral mass, and energy content in carcass more precisely than carcass weight alone did, resulting in a maximum decreased rCV of –1% for lipid mass. The water mass and energy amount in carcass were the only carcass components where US variable was significant. Among the in vivo methods tested, only US provided better relationships than BW alone (not considering the 3D imaging method, only measured in 8 cows). Water carcass mass was estimated with a rCV of 4% and energy carcass content with a rCV 9%. Among the post mortem methods tested, perirenal ACS was the least accurate. Conversely, the use of the 11th rib dissection with carcass weight or BW was a very accurate method. The cannon bone and perirenal AT masses decreased the rCV by another –0.3% for energy content in carcass when added to the 11th rib dissection variables and carcass weight. Adding

**Table 2.** Carcass and 11th rib cut measurements of 6 primiparous and 6 multiparous Simmental cows ($n$ = 12) and calves ($n$ = 10) at 288 days in milk or old, respectively

| | All | | | | Cows | | | | Calves | | | |
|---|---|---|---|---|---|---|---|---|---|---|---|---|
| | Mean | SD | Min | Max | Mean | SD | Min | Max | Mean | SD | Min | Max |
| Anatomical weights, kg | | | | | | | | | | | | |
| Perirenal adipose tissue | 8.2 | 3.2 | 2.4 | 15.8 | 9.2 | 3.5 | 4.7 | 15.8 | 6.9 | 2.3 | 2.4 | 9.8 |
| Left rear metacarpus or cannon bone | 0.69 | 0.12 | 0.52 | 0.92 | 0.76 | 0.10 | 0.56 | 0.92 | 0.61 | 0.07 | 0.52 | 0.75 |
| Left front metacarpus or cannon bone | 0.65 | 0.10 | 0.47 | 0.78 | 0.71 | 0.04 | 0.64 | 0.78 | 0.57 | 0.08 | 0.47 | 0.69 |
| Morphological measurements, cm | | | | | | | | | | | | |
| Carcass total length | 246.2 | 40.4 | 111.5 | 285.0 | 273.3 | 9.1 | 258.0 | 285.0 | 210.1 | 37.4 | 111.5 | 229.0 |
| Length between the hook and pubic symphysis | 80.2 | 6.4 | 71.0 | 88.5 | 85.3 | 2.1 | 82.5 | 88.5 | 73.3 | 1.7 | 71.0 | 75.5 |
| Thigh thickness | 26.3 | 3.2 | 18.8 | 29.8 | 28.5 | 1.3 | 26.5 | 29.8 | 23.4 | 2.5 | 18.8 | 28.0 |
| Compactness index (Thigh thickness/ Length between the hook and pubic symphysis) | 0.33 | 0.03 | 0.26 | 0.38 | 0.33 | 0.02 | 0.30 | 0.35 | 0.32 | 0.03 | 0.26 | 0.38 |
| Subcutaneous adipose tissue thickness average, cm measured by ultrasound | 0.69 | 0.42 | 0.17 | 1.82 | 0.88 | 0.47 | 0.17 | 1.82 | 0.46 | 0.19 | 0.25 | 0.76 |
| Subcutaneous adipose cell size, µm | 122.9 | 14.4 | 90.1 | 141.5 | 123.8 | 16.3 | 90.1 | 141.5 | 121.9 | 12.5 | 103.9 | 137.7 |
| Carcass dual-energy X-ray absorptiometry scan, kg | | | | | | | | | | | | |
| Total mass | 121.61 | 32.63 | 69.69 | 164.69 | 149.02 | 12.16 | 131.85 | 164.69 | 88.73 | 10.04 | 69.69 | 101.59 |
| Lean mass | 97.64 | 25.92 | 60.57 | 134.48 | 119.57 | 8.80 | 105.72 | 134.48 | 71.34 | 7.94 | 60.57 | 85.10 |
| Fat mass | 17.67 | 5.97 | 5.86 | 29.97 | 21.42 | 4.96 | 12.30 | 29.97 | 13.18 | 3.46 | 5.86 | 19.89 |
| Bone mineral content mass | 6.30 | 2.00 | 3.27 | 9.33 | 8.03 | 0.58 | 6.92 | 9.33 | 4.22 | 0.36 | 3.27 | 4.50 |
| 11th rib dissection, g | | | | | | | | | | | | |
| Total weight | 1,016 | 276 | 248 | 1,397 | 1,211 | 126 | 1,043 | 1,397 | 781 | 214 | 248 | 936 |
| Adipose tissue weight | 231 | 65 | 92 | 368 | 259 | 64 | 150 | 368 | 198 | 51 | 92 | 263 |
| Muscle weight | 610 | 144 | 371 | 866 | 722 | 74 | 604 | 866 | 476 | 69 | 371 | 576 |
| Bone weight | 195 | 43 | 136 | 260 | 228 | 27 | 173 | 260 | 156 | 19 | 136 | 184 |
| 11th rib cut dual-energy X-ray absorptiometry scan, g | | | | | | | | | | | | |
| Total mass | 1,021 | 221 | 660 | 1,374 | 1,191 | 122 | 1,029 | 1,374 | 817 | 103 | 660 | 918 |
| Lean mass | 676 | 150 | 416 | 941 | 792 | 76 | 661 | 941 | 537 | 78 | 416 | 666 |
| Fat mass | 289 | 83 | 127 | 465 | 328 | 83 | 191 | 465 | 243 | 55 | 127 | 320 |
| Bone mineral content mass | 55 | 18 | 28 | 84 | 71 | 8 | 54 | 84 | 37 | 5 | 28 | 42 |

**Table 3.** Morphological traits of eight Simmental cows measured via three-dimensional imaging

| Item | Mean | SD | Min | Max |
|---|---|---|---|---|
| Volume and surface | | | | |
| Partial volume, L | 597.9 | 56.3 | 528.6 | 655.4 |
| Partial surface, $m^2$ | 5.2 | 0.3 | 4.8 | 5.6 |
| Linear measurements, cm | | | | |
| Wither height | 141.5 | 2.9 | 137.4 | 145.4 |
| Hip height | 142.2 | 3.2 | 139.3 | 148.4 |
| Back length between wither and sacrum | 86.9 | 6.4 | 73.7 | 94.6 |
| Hip width | 54.7 | 2.5 | 50.8 | 57.5 |
| Chest depth | 78.5 | 2.6 | 75.1 | 81.7 |
| Heart girth | 209.8 | 4.7 | 205.8 | 218.6 |
| Diagonal length between left shoulder and right ischium | 162.5 | 10.2 | 147.5 | 183.0 |
| Diagonal length between right shoulder and left ischium | 163.3 | 7.2 | 152.9 | 176.2 |

**Table 4.** Most accurate estimative equations predicting empty body chemical component mass from body weight and independent variables ($P < 0.10$) derived from adipose cell diameter (μm) and subcutaneous adipose tissue thickness ultrasound measurement (cm)

| Chemical components | Equations | Statistics | | |
|---|---|---|---|---|
| | | RMSEP | $R^2$ | rCV |
| Water, kg | | | | |
| Body weight | (70.373, 41.811) + 0.398 × BW* | 9.8 | 0.976 | 3.9 |
| Adipose cell diameter | 47.692 + 0.518 × BW–0.393 × ACS subcutaneous* | 9.1 | 0.979 | 3.6 |
| Ultrasound | (62.637, 36.315) + 0.430 × BW–12.874 × AT thickness* | 8.7 | 0.981 | 3.5 |
| Lipids, kg | | | | |
| Body weight | (–109.330, –61.002) + 0.331 × BW* | 12.4 | 0.688 | 17.1 |
| Adipose cell diameter | (–111.908, –82.618) + 0.247 × BW + 0.423 × ACS subcutaneous* | 11.3 | 0.743 | 15.6 |
| Ultrasound | (–54.304, –145.496) + 0.292 × BW + 15.692 × AT thickness* | 11.2 | 0.747 | 15.4 |
| Proteins, kg | | | | |
| Body weight | 5.605 + 0.137 × BW* | 2.8 | 0.973 | 3.9 |
| Minerals, kg | | | | |
| Body weight | (7.833, 4.187) + 0.020 × BW* | 1.1 | 0.936 | 6.9 |
| Energy, MJ | | | | |
| Body weight | (–3933.610, –2174.680) + 15.744 × BW* | 486.3 | 0.840 | 10.9 |
| Adipose cell diameter | –2309.920 + 8.396 × BW + 22.148 × ACS subcutaneous* | 450.3 | 0.862 | 10.1 |
| Ultrasound | (–3575.190, –1920.060) + 14.244 × BW + 596.443 × AT thickness* | 445.9 | 0.865 | 10.0 |

Abbreviations: adipose cell size (ACS), adipose tissue (AT), bone mineral content (BMC), body weight (BW), hot carcass weight (CW), dual-energy X-ray absorptiometry (DXA), residual coefficient of variation (rCV; ratio of RMSEP to the mean of the dependant variable) and root mean square error of prediction (RMSEP). The AT thickness measured by ultrasound is the average between the minimum and maximum thickness measured.
*Indicates that the intercept is significantly different from 0 ($P < 0.05$) and italic variables indicate a tendency ($0.10 > P > 0.05$). When place into brackets, the intercept was different ($P < 0.05$ or $P < 0.10$ when italic) according to the animal type and are presented in the following order: cows, calves.

cannon bone mass and thigh thickness to the 11th rib dissection variables and BW decreased the rCV by –0.9% for mineral mass.

The half-carcass DXA scan was the most accurate method among all methods tested, with a reduction of the rCV compared to the BW or carcass weight alone of –12% for carcass lipid mass, –4% for carcass water mass, –3% for carcass mineral mass, –2% for carcass protein mass, and –8% for carcass energy content. The accuracy of the chemical component estimation by the 11th rib scan DXA was very close to the estimation by the half-carcass DXA scan, showing only a decrease in accuracy of +2.5% rCV for carcass lipid mass, +1.3% for carcass energy content, +0.5% for carcass water mass, and +0.2% for carcass protein mass.

## Estimation of the Cow Empty Body and Carcass Chemical Component Masses by Three-dimensional Imaging

Using a simple linear regression with partial volume of the 8 cows, the BW was estimated with $R^2 = 0.83$, RMSEP = 21 kg, and a rCV = 3%.

The results of the EB and carcass chemical components estimated by PLS regressions using 10 variables harvested by 3D imaging on 8 cows are presented in Table 6, Supplementary Tables S2 and S3. Empty body water, lipid, and protein masses were estimated with a PLS regression including the first six latent variables, with similar $R^2$ superiority of 0.990, regardless of the inclusion of BW. Empty body water and protein mass estimations had a residual coefficient of variation less

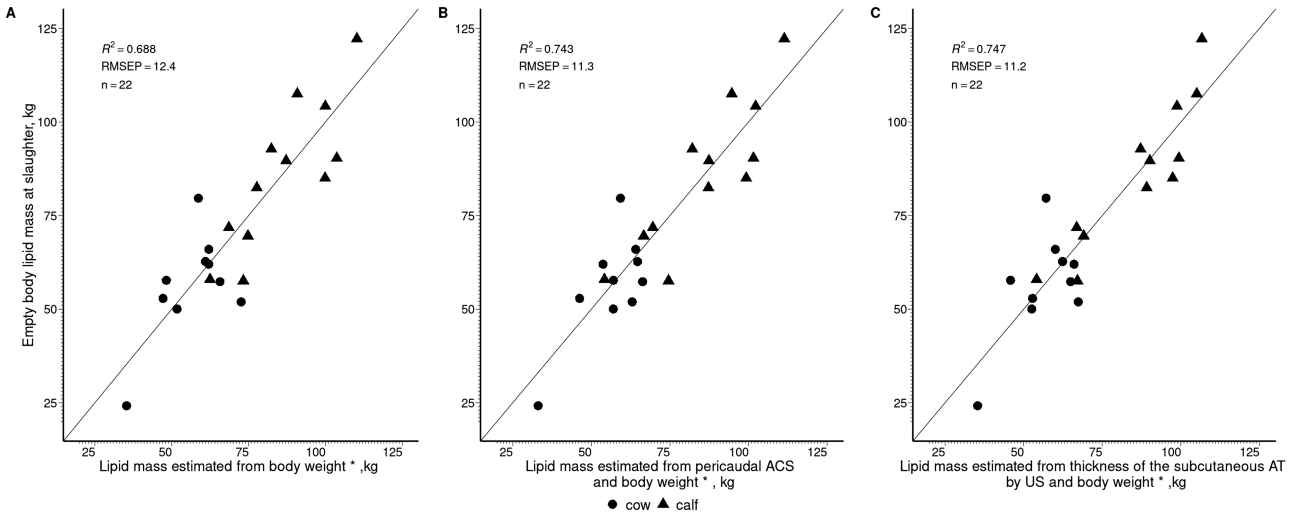


**Figure 3.** Plots of relationships for the most accurate relationships between measured empty body lipid mass of Simmental cows and calves and its estimation from multiple regression equations developed from A) body weight alone, or body weight together with B) adipose cell size and C) ultrasound backfat thickness. RMSEP: root mean square error of prediction; ACS: adipose cell size; AT: adipose tissue; US: ultrasound; * indicates an animal type (cow or calf) effect on the intercept.

than 5%, while EB lipid mass had a coefficient of 17%; the latter being the most important parameter in estimating EB chemical amounts. Energy content and mineral mass had the smallest $R^2$, only explained by one latent variables. Empty body energy content was explained most accurately by 3D variables and BW ($R^2$ = 0.791; rCV = 15.4%) than by only 3D variables ($R^2$ = 0.758; rCV = 16.5%). Minerals were the component with the smallest $R^2$ of around 0.650, but the rCV was only 8%, resulting in an error of 1.2 kg.

Carcass lipid and protein masses, as well as energy, were estimated by PLS regression models including six latent variables (Table 6 and Supplementary Table S2), while only four were needed for the carcass water and one for mineral mass. For these models, $R^2$ ranged from 0.728 for carcass mineral mass estimation without BW to 0.999 for carcass protein mass estimation with BW. The models' RMSEP with or without BW were very close for each variable between both models. The rCV was 7% for carcass mineral mass between models. For carcass protein mass, rCV was 5.6% for the model with BW and 6.1% for the model without BW. Carcass lipid mass was estimated with the rCV of 21.2% for the model with BW and 21.9% for the model without BW. The rCV for the carcass water mass was 6.2% for the model with BW and 6.8% for the model without BW. Carcass energy content was predicted with an RMSEP of 259 MJ with BW and 290 MJ without BW, the rCV varying between 10% and 11%.

## DISCUSSION

Few studies have compared several methods aimed at estimating body chemical composition in cattle. The present study indicates that DXA and 3D imaging technologies are interesting alternative methods to other established and well-known methods (ACS, US, and rib dissection) for the in vivo and post mortem estimation of body and carcass compositions. Our results also suggest that they are accurate in both adult (lactating cows) or growing (heifers and steers) bovine of Simmental breed.

Fat-free EB chemical composition did not depend on animal type, which was found to be in agreement with results from Yan et al. (2009) and Fiems et al. (2005). Lerch et al. (2015, 2021) found similar values for fat-free EB composition (72% to 76% of water, 20% to 23% of proteins, and 4% to 7% of minerals) in goats. Additionally, both subcutaneous and perirenal ACS were similar in calves and cows, in accordance with the similarly recorded body fatness. The subcutaneous ACS found in this study was higher than those reported by Robelin (1981; 80 µm and 100 µm in Pie Noire and Charolais bulls), Hood and Allen (1973; 75 µm to 138 µm in 14 mo Hereford or Hereford × Angus cattle), and de la Torre-Capitan et al. (2015; 53 µm to 86 µm in Charolais cows). However, this value was smaller than those reported by Waltner et al. (1994; 144 µm in lactating dairy cows). Similarly, Hood and Allen (1973) and Waltner et al. (1994) recorded slightly smaller perirenal ACS than in the present study. According to Hood and Allen (1973), the unimodal distribution, and absence of small cells (<70 µm), as in the present study, is a good indicator of non-late cellular hyperplasia in AT. Robelin (1981) noticed that primary hyperplasia occurs until growing male cattle reach a BW of around 45% of adult weight. This BW was reached at one year of age for Pie Noire and Charolais bulls (Robelin, 1981), whereas the growing heifers and steers of the present study reached around 60% of their mother's weight at 10 mo.

The BW explained the major part of the variation in EB or carcass water, protein, and mineral masses, providing results close to those obtained when adding in vivo method variables to the estimative relationships. Conversely, for lipid mass, the accuracy of the equation with BW was improved by adding some variables derived of methods such as ACS. Similarly, Waltner et al. (1994) improved the prediction of the amount of AT in EB with BW and subcutaneous ACS together by decreasing the error by −3 kg, compared to BW alone. When using perirenal ACS, the error was further lowered by −5 kg (Waltner et al., 1994). In the present study, the perirenal ACS in vivo sampling is the most invasive method among all the methods presented in this study for monitoring living cattle. Nonetheless, the use of perirenal ACS compared to

**Table 5.** Most accurate estimative equations predicting carcass chemical component mass from body weight or carcass weight and independent variables ($P < 0.10$) derived from adipose cell diameter (μm), subcutaneous adipose tissue thickness ultrasound measurement (cm), 11th rib dissection (g), anatomical measurements, 11th rib cut dual energy X-ray absorptiometry (DXA; g) and carcass DXA scan (kg). When significant ($P < 0.05$), body weight or carcass weight was included as second predictive variable in the multiple linear regression

| Chemical component | Equations | Statistics | | |
|---|---|---|---|---|
| | | RMSEP | $R^2$ | rCV |
| Water, kg | | | | |
| Body weight | 0.283 + 0.308 × BW | 7.8 | 0.959 | 5.2 |
| Carcass weight | (33.751, 20.567) + 0.496 × CW | 6.4 | 0.973 | 4.3 |
| Ultrasound | (30.882, 18.466) + 0.526 × CW − 6.867 × *AT thickness* | 6.0 | 0.976 | 4.0 |
| Adipose cell diameter | 27.338 + 0.610 × CW − 0.191 × ACS perirenal* | 5.7 | 0.979 | 3.8 |
| 11th rib cut dissection | −3.133 + 0.452 × CW −0.067 × 11th rib muscle mass − 0.065 × 11th rib AT mass + 0.088 × 11th rib bone mass | 3.3 | 0.993 | 2.2 |
| 11th rib cut DXA scan | 0.738 − 4.44 × $10^{-5}$ × fat mass + 2.72 × $10^{-4}$ × BMC mass + 5.39 × $10^{-5}$ × lean mass + 0.449 × CW | 3.0 | 0.994 | 2.0 |
| Carcass DXA scan | 3.121 − 1.689 × fat mass + 0.719 ×CW | 2.3 | 0.996 | 1.5 |
| Lipids, kg | | | | |
| Carcass weight | (−45.429, −27.259) + 0.321 × CW* | 7.0 | 0.745 | 17.0 |
| Body weight | (−57.793, −35.503) + 0.184 × BW* | 6.6 | 0.773 | 16.0 |
| Adipose cell diameter | −32.630 + 0.088 × BW + 0.218 × ACS perirenal* | 6.4 | 0.790 | 15.6 |
| 11th rib cut dissection | −0.218 + 0.302 × CW − 0.066 × 11th rib muscle mass + 0.089 × 11th rib AT mass + *0.065 × 11*th *rib bone mass* | 3.9 | 0.921 | 9.5 |
| 11th rib cut DXA scan | −3.671 + 2.38 × $10^{-4}$ × lean mass + 3.56 × $10^{-4}$ × fat mass + 0.310 × CW − 0.289 × total mass by DXA | 2.9 | 0.956 | 7.1 |
| Carcass DXA scan | −4.699 −1.841 × lean mass −3.722 × BMC mass + 2.071 × half-carcass scanned mass* | 1.9 | 0.980 | 4.6 |
| Proteins, kg | | | | |
| Body weight | 0.524 + 0.087 × BW | 2.3 | 0.955 | 5.4 |
| Carcass weight | 1.530 + 0.168 × CW | 1.8 | 0.974 | 4.2 |
| 11th rib cut dissection | 2.924 + 0.180 × CW − 0.019 × 11th rib AT mass* | 1.6 | 0.980 | 3.8 |
| 11th rib cut DXA scan | 2.798 − 1.64 × $10^{-5}$ × fat mass + 0.182 × CW* | 1.5 | 0.981 | 3.5 |
| Carcass DXA scan | 1.155 − 0.348 × fat mass + 0.396 × half-carcass scanned mass | 1.4 | 0.983 | 3.3 |
| Minerals, kg | | | | |
| Carcass weight | (6.188, 3.144) + 0.027 × CW* | 0.9 | 0.921 | 7.9 |
| Body weight | (4.567, 2.101) + 0.016 × BW | 0.9 | 0.931 | 7.9 |
| 11th rib cut dissection | (5.232, 2.730) + 0.022 × BW − 0.005 × *11*th *rib muscle mass* | 0.8 | 0.939 | 7.0 |
| Anatomical measurements | (4.034, −0.698) + 2.102 × cannon bone total mass − 0.005 × 11th rib muscle mass + 0.010 × 11th rib AT mass + 0.181 × *thigh thickness* | 0.7 | 0.951 | 6.2 |
| Carcass DXA scan | 0.731 + 0.070 × fat mass + 1.492 × BMC mass | 0.6 | 0.962 | 5.3 |
| Energy, MJ | | | | |
| Carcass weight | (−1593.526, −971.350) + 15.998 × CW | 252.9 | 0.894 | 9.7 |
| Body weight | (−2065.536, −1295.504) + 8.935 × BW | 244.2 | 0.901 | 9.4 |
| Ultrasound | (−1916.796, −1189.840) + 8.312 × BW + 247.516 × *AT thickness** | 236.3 | 0.907 | 9.1 |
| Adipose cell diameter | −1164.783 + 10.701 × CW + 7.980 × ACS perirenal* | 226.1 | 0.915 | 8.7 |
| 11th rib cut dissection | 26.581 + 16.328 × CW − 2.527 × 11th rib muscle mass + 3.048 × 11th rib AT mass − 2.971 × 11th rib bone mass | 133.6 | 0.970 | 5.1 |

**Table 5.** Continued

| Chemical component | Equations | Statistics | | |
|---|---|---|---|---|
| | | RMSEP | $R^2$ | rCV |
| Anatomical measurements | (−451.281, −75.287) + 19.469 × CW + 39.624 × perirenal AT mass − 261.309 × cannon bone total mass −2.463 × 11th rib muscle mass | 125.6 | 0.974 | 4.8 |
| 11th rib cut DXA scan | −136.064 + 2.19 × $10^{-3}$ × fat mass − 1.22 × $10^{-2}$ × BMC mass + 16.815 × CW − 1.97 × $10^{-3}$ × lean mass | 91.1 | 0.986 | 3.5 |
| Carcass DXA scan | (11.145, 447.359) + 71.940 × fat mass − 117.911 × BMC mass + 7.933 × CW | 56.8 | 0.995 | 2.2 |

Abbreviations: adipose cell size (ACS), adipose tissue (AT), bone mineral content (BMC), body weight (BW), hot carcass weight (CW), dual-energy X-ray absorptiometry (DXA), residual coefficient of variation (rCV; ratio of RMSEP to the mean of the dependant variable) and root mean square error of prediction (RMSEP). The AT thickness measured by ultrasound is the average between the minimum and maximum thickness measured.
*Indicates that the intercept is significantly different from 0 ($P < 0.05$) and italic variables indicate a tendency ($0.10 > P > 0.05$). When place into brackets, the intercept was different ($P < 0.05$ or $P < 0.10$ when italic) according to the animal type and are presented in the following order: cows, calves.

subcutaneous ACS provided more accurate predictions for EB lipid mass ($R^2$ =0.78 and RMSEP = 10 kg). The use of US provided better results in predicting the different chemical component amounts compared to ACS in the present study, conversely to previous investigations in dairy goats (Lerch et al., 2021). The correlation (Supplementary Table S4) between US backfat thickness and EB lipid mass of +0.67 was within the interval of +0.28 to +0.94 reported by Schröder and Staunfenbiel (2006), whereas the correlation between carcass lipid mass and US backfat thickness of +0.62 was higher than the +0.54 value reported by Bruckmaier et al. (1998) for the relationship with dissected carcass AT.

The 3D variables were tested to estimate the in vivo chemical composition of the carcass or EB. Fonseca et al. (2017) estimated the carcass lipid mass with an error of 7 kg and 12 kg for the EB lipid mass, with body measurements manually recorded in intact or castrated crossbred Angus × Nellore male, which is less important than in the present study. The rCV obtained by Fonseca et al. (2017) was less than 15% (17% minimum in present study). Gomes et al. (2016) noticed a rCV of 9% on Angus bulls and 10% on Angus and Nellore bull groups for the prediction of the proportion of lipids in the EB, but with a lower $R^2$ value (0.43 to 0.45) than in the present study (11% of variation for the error and $R^2$ of 0.997). However, the lipids proportions contained in EB were less variable for Gomes et al. (2016) than in the present study.

The BW was estimated with $R^2$ = 0.83 and a RMSEP = 21 kg with a simple linear regression with partial volume of 8 cows. The 3D imaging has already been used to estimate carcass weight and BW (Gomes et al. 2016; Miller et al. 2019). Miller et al. (2019) estimated BW using either a linear regression approach ($R^2$ = 0.70 and RMSE = 42 kg) or artificial neural network [$R^2$ = 0.54 and RMSE = 51 kg (rCV = 8%)]. Gomes et al. (2016) used multiple regression approaches and published even more accurate equations to estimate BW ($R^2$ = 0.84, RMSE = 19 kg and rCV = 4% on an Angus and Nellore cattle group; $R^2$ = 0.76, RMSE = 23 kg and rCV = 5% on an Angus group). All these authors used 3D depth cameras placed on the top of animals that appear to be easier to use on-farm. However, the accuracy and the feasibility of several measurements allowed by the full body 3D scan performed in the present study are mandatory for the development of accurate estimative equations in a research context.

In terms of cost, time, and invasiveness, among all in vivo methods tested in the present study, the ACS is the most difficult to implement because of material to be used, the time to obtain results, the invasiveness regardless of the targeted tissue, the expertise required, and the sampling procedures, as well as possible risks for both animal and human health. The US can be performed on-site and is noninvasive, but required a specific equipment and concomitant expertise, especially regarding the human effect on the images capture and treatment, which are operator dependent. The 3D imaging allows to overpass the problems of expertise and human effect especially with the automation of image capture. However, the equipment used in the present study is a prototype only usable currently in the research field.

The methods tested for the post mortem estimation of the carcass chemical composition (DXA and rib dissection) were more accurate than the estimations based on in vivo indicators (US and ACS). The DXA scan of half-carcass is the most accurate method tested to predict

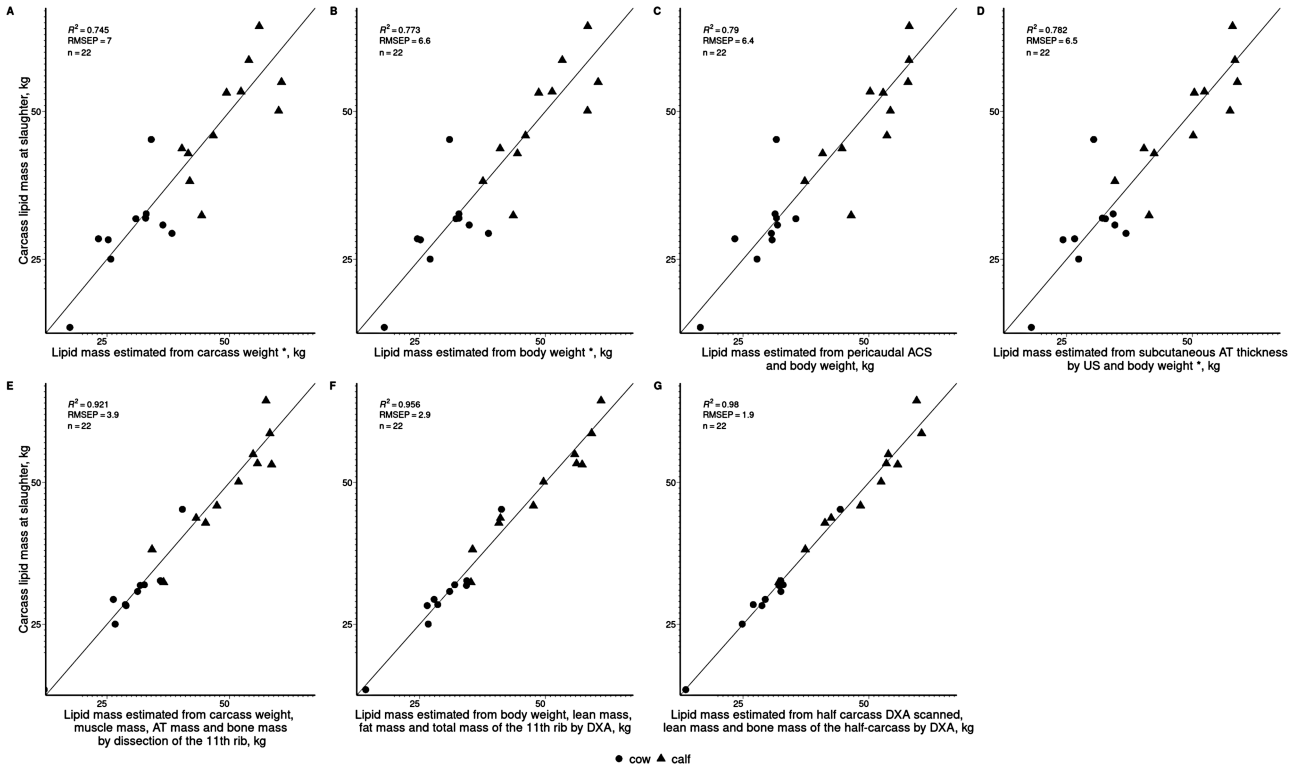


**Figure 4.** Plots of relationships for the most accurate relationship between measured carcass lipid mass of Simmental cows and calves and its estimation form multiple regression equations developed from A) carcass weight, B) body weight, C) adipose cell size, D) ultrasound backfat thickness, E) dissection of the 11th rib cut, F) dual-energy X-ray absorptiometry scan of the 11th rib cut, and G) dual-energy X-ray absorptiometry scan of the half-carcass. When significant ($P < 0.05$), body weight or carcass weight was included as a second predictive variable in the multiple linear regression. RMSEP: root mean square error of prediction; ACS: adipose cell size; AT: adipose tissue; US: ultrasound; * indicates an animal type (cow or calf) effect on the intercept.

**Table 6.** Most accurate partial least square (PLS) estimative regressions for the empty body and carcass chemical component mass measured after slaughter using body weight and independent variables derived from morphological measurements obtained with three-dimensional imaging and body weight of 8 Simmental cows

| Chemical component | Empty body | | | | Carcass | | | |
|---|---|---|---|---|---|---|---|---|
| | No. of latent variables | RMSEP | $R^2$ | rCV | No. of latent variables | RMSEP | $R^2$ | rCV |
| Water, kg | | | | | | | | |
| M1 + body weight | 6 | 7.7 | 0.9993 | 3.1 | 4 | 9.2 | 0.9856 | 6.2 |
| M1 | 6 | 9.8 | 0.9997 | 3.9 | 4 | 10.1 | 0.9721 | 6.8 |
| Lipids, kg | | | | | | | | |
| M1 + body weight | 6 | 12.3 | 0.9982 | 17.0 | 6 | 8.7 | 0.9969 | 21.2 |
| M1 | 6 | 12.3 | 0.9970 | 17.0 | 6 | 9.0 | 0.9964 | 21.9 |
| Proteins, kg | | | | | | | | |
| M1 + body weight | 6 | 3.5 | 0.9991 | 4.9 | 6 | 2.4 | 0.9995 | 5.6 |
| M1 | 6 | 3.5 | 0.9993 | 4.9 | 6 | 2.6 | 0.9990 | 6.1 |
| Minerals, kg | | | | | | | | |
| M1 + body weight | 1 | 1.2 | 0.6486 | 7.5 | 1 | 0.8 | 0.7279 | 7.0 |
| M1 | 1 | 1.2 | 0.6559 | 7.5 | 1 | 0.8 | 0.7304 | 7.0 |
| Energy, MJ | | | | | | | | |
| M1 + body weight | 1 | 687 | 0.7911 | 15.4 | 6 | 259 | 0.9990 | 10.0 |
| M1 | 1 | 737 | 0.7582 | 16.5 | 6 | 290 | 0.9988 | 11.2 |

Abbreviations: root mean square error of prediction (RMSEP); % variance of the outcome variable explained by components ($R^2$) and residual coefficient of variation (rCV; ratio of RMSEP to the mean of the dependant variable).
M1: Partial volume, partial surface, wither height, hip height, back length between wither and sacrum, chest depth, hip width, heart girth, the 2 diagonal length between shoulder and the opposite ischium.

chemical composition of every chemical component. The DXA technology was calibrated for different breed types (purebred or crossbred) without observing breed effect on relationships for the estimation of carcass tissue composition (i.e., AT, muscles, and bone masses) using anatomical dissection (López-Campos et al., 2018; Segura et al., 2021) or computer tomography (Calnan et al., 2021) as a "gold standard" reference. Depending on the considered equations, the external validation performed by López-Campos et al. (2018) reached $R^2$ from 0.93 to 0.99 for muscle mass, 0.74 to 0.98 for AT mass, and 0.60 to 0.94 for bone mass. The error reported as a percentage was maximum 2%. This error is slightly lower than the one reported in present study, presumably due to the difference in predicted composition [chemical in the present study and tissue in López-Campos et al. (2018)], statistical methods [multiple linear regression in the present study and PLS regression in López-Campos et al. (2018)], validation methods [leave-one-out-cross-validation in the present study and external validation dataset in López-Campos et al. (2018)], and DXA devices. Although the half-carcass DXA scan is the most accurate method to estimate the carcass' composition, it remains time consuming when dealing with large pieces and requires an expensive device. Still, using DXA in commercial slaughterhouses for beef carcass grading was initiated by Calnan et al. (2021) and Segura et al. (2021). The use of such techniques at slaughterhouse line speed was, however, confronted with the technical challenge to develop a DXA device appropriate for a whole beef half-carcass, as realized for sheep (Gardner et al., 2018; Connaughton et al., 2021). The use of only a part of the carcass, such as a rib section or a single rib, could be an option to face this challenge.

The estimation of the carcass' composition based on the dissection of one rib together with slaughter measurements provided a simple and accurate method, as previously outlined by Robelin et al. (1976). Fiems et al. (2005) with the 8th rib dissection and Berndt et al. (2017) with the 9th to 11th ribs dissections concluded similarly to Robelin et al. (1976), who outlined the effect of the breed on the intercept, similar to the effect of the animal type (cow/calf) in the present study. The interest is that when only a part of the carcass is used to estimate the whole composition, it saves time and alleviates the destruction of the whole carcass. However, dissection asks for the intervention of a specialized butcher, which means that the final result is still influenced by operator. Besides, this method requires around 15 min per rib. Recently, Meunier et al. (2021) tested image analysis on the 6th rib to limit the destruction, reduce time for estimation, and alleviate operator effect. Another imaging alternative, is the rib DXA scan, as tested in the present study. It appeared to be the second most accurate method, besides the half-carcass DXA scan, to predict the carcass chemical composition, except for minerals, for which no equation could be set-up. The DXA, is non-destructive (i.e., carcass or rib cut scanned remains intact and further saleable), but requires an expensive equipment and requires less than 5 min of scan for single rib cut, but until 40 min for a half-carcass. Contrary to others devices as CT or MRI, specific expertise is not necessary with DXA because the acquisition is automatic and images treatment does not need specific skills and is operator independent. Moreover, the level of radiation of DXA is lower than when using CT.

## CONCLUSIONS

This study compared different in vivo and post mortem methods for the estimation of EB or carcass chemical compositions in lactating cows and their offspring. Among the methods tested, US was the most accurate in vivo method, except for protein masses with no improvement when including subcutaneous AT thickness variable over BW alone. Among all post mortem methods, the DXA scan of the half-carcass was the best method to estimate its chemical composition. Use of 11th rib dissected or DXA scanned also provided an accurate estimation of carcass chemical composition, with slightly less accurate estimations via dissection than with DXA scan. Besides, dissection requires butcher skills and time. In the conditions of the present study, the ACS resulted in the least accurate relationships for estimating the EB and carcass composition. This method also required technicity and is quite invasive. The results obtained with 3D imaging are promising. This method combines noninvasive procedures, reduces animal handling, and allows access to many morphological phenotypes. Future research is required to test 3D imaging on a larger sample size of cattle of different breeds in order to confirm and improve its accuracy. Present study indeed included a limited number of animals and one breed, but provided useful results positioning the relative accuracy of different methods to estimate chemical composition of empty body and carcass. Increasing the number of animals in future research, with different breeds and physiological states, could guarantee the results and open up new possibilities by focusing on the most promising methods such as 3D or DXA. At long term, the on-farm in vivo monitoring of the lipid reserves, protein accretion, or skeletal development may allow the dynamic defining of individual nutritional requirements, and improve animal robustness and feed efficiency. Wide implications may therefore be expected in animal research and ultimately for precision livestock farming implementation in commercial farms.

## Supplementary Data

Supplementary data are available at *Translational Animal Science* online.

## Acknowledgments

We thank Y. Aeby and the team of the Posieux Experimental Barn of Agroscope for diligent feeding, milking, and management of cows and calves; B. Egger, F. Sansonnens and G. Maikoff for slaughter and empty body mincing procedures; S. Dubois and all the feed chemistry unit of Agroscope (Posieux, Switzerland) for empty body and carcass chemical analyses. C.X. acknowledges the financial support of a Ph.D. studentship provided by Agrocampus-Ouest (Rennes, France) and Institut national de recherche pour l'agriculture, l'alimentation et l'environnement (INRAE; department of Animal Physiology and Livestock Systems; Paris, France). We thank the program Hubert Curien (PHC) Germaine de Staël between France and Switzerland for funding awarded to support mobility of partners along the project 2021–20 CompoMeat 3D. We thank Scribendi (Chatham, ON, Canada) for the proof reading.

## Conflict of interest statement

The authors declare no conflicts of interest.

## Literature Cited


Bergen, R., S. P. Miller, I. B. Mandell, and W. M. Robertson. 2005. Use of live ultrasound, weight and linear measurements to predict carcass composition of young beef bulls. *Can. J. Anim.* 85:23–35. doi:10.4141/A04-011

Berndt, A., D. P. D. Lanna, G. M. da Cruz, R. R. Tullio, L. S. Sakamoto, and M. M. de Alencar. 2017. Prediction of the chemical body composition of Nellore and crossbreed bulls. *J. Anim. Sci.* 95:3932–3939. doi:10.2527/jas2017.1484

Bruckmaier, R. M., E. Lehmann, D. Hugi, H. M. Hammon, and J. W. Blum. 1998. Ultrasonic measurements of longissimus dorci muscle and backfat associated with metabolic and endocrine traits, during fattening of intact and castrated male cattle. *Livest. Prod. Sci.* 53:123–124. doi:10.1016/S0301-6226(97)00162-0

Calnan, H., A. Williams, J. Peterse, S. Starling, J. Cook, S. Connaughton, and G. E. Gardner. 2021. A prototype rapid dual energy X-ray absorptiometry (DEXA) system can predict the CT composition of beef carcasses. *Meat Sci.* 173:1–12. doi:10.1016/j.meatsci.2020.108397

Cominotte, A., A. F. A. Fernandes, J. R. R. Dorea, G. J. M. Rosa, M. M. Ladeira, E. H. C. B. van Cleef, G. L. Pereira, W. A. Baldassini, and O. R. Machado Neto. 2020. Automated computer vision system to predict body weight and average daily gain in beef cattle during growing and finishing phases. *Livest. Sci.* 232:1–10. doi:10.1016/j.livsci.2019.103904

Connaughton, S. L., A. Williams, F. Anderson, K. R. Kelman, J. Peterse, and G. E. Gardner. 2021. Dual energy X-ray absorptiometry predicts lamb carcass composition at abattoir chain speed with high repeatability across varying processing factors. *Meat Sci.* 181:108413. doi:10.1016/j.meatsci.2020.108413

De la Torre-Capitan, A., E. Recoules, F. Blanc, I. Ortigues Marty, P. d'Hour, and J. Agabriel. 2015. Changes in calculated residual energy in variable nutritional environments: an indirect approach to apprehend suckling beef cows' robustness. *Livest. Sci.* 176:75–84. doi:10.1016/j.livsci.2015.03.008

Driesen, C., S. Lerch, R. Siengenthaler, P. Silacci, H. D. Hess, B. Nowack, and M. Zennegg. 2022. Accumulation and decontamination kinetics of PCBs and PCDD/Fs from grass silage and soil in a transgenerational cow-calf setting. *Chemosphere*. 296:133951. doi:10.1016/j.chemosphere.2022.133951

Fiems, L. O., W. Van Caelenbergh, J. M. Vanacker, S. De Campeneere, and M. Seynaeve. 2005. Prediction of empty body composition of double-muscled beef cows. *Livest. Prod. Sci.* 92:249–259. doi:10.1016/j.livprodsci.2004.09.002

Fonseca, M. A., L. O. Tedeschi, S. Valadares Filho, N. F. De Paula, F. A. C. Villadiego, J. Silva Junior, D. C. Abreu, and M. L. Chizzotti. 2017. Assessment of body fat composition in crossbred Angus x Nellore using biometric measurements. *J. Anim. Sci.* 95:5584–5596. doi:10.2527/jas2017.1840

Fox, J., and S. Weisberg. 2019. *An {R} companion to applied regression*. 3rd ed. Thousand Oaks (CA): Sage. Available from https://socialsciences.mcmaster.ca/jfox/Books/Companion/

Gardner, G. E., S. Straling, J. Charnley, J. Hocking-Edwards, J. Peterse, and A. Williams. 2018. Calibration of an on-line dual energy X-ray absorptiometer for estimating carcase composition in lamb at abattoir chain-speed. *Meat Sci.* 144:91–99. doi:10.1016/j.meatsci.2018.06.020

Geay, Y., and C. Béranger. 1969. Estimation de la composition de la carcasse de jeunes bovins à partir de la composition d'un morceau monocostal au niveau de la 11ème côte. *Ann. Zootech.* 18:65–77. doi:10.1051/animres:19690106. https://hal.archives-ouvertes.fr/hal-00886957/document.

Greiner, S. P., G. H. Rouse, D. E. Wilson, L. V. Cundiff, and T. L. Wheeler. 2003. Accuracy of predicting weight and percentage of beef carcass retail product using ultrasound and live animal measures. *J. Anim. Sci.* 81:466–473. doi:10.2527/2003.812466x

Gomes, R. A., G. R. Monteiro, G. L. Assis, K. C. Busato, M. M. Ladeira, and M. L. Chizzotti. 2016. Technical note: estimating body weight and body composition of beef cattle trough digital image analysis. *J. Anim. Sci.* 94:5414–5422. doi:10.2527/jas.2016-0797

Hankins, O. G., and P. E. Howe. 1946. Estimation of the composition of beef carcasses and cuts. *USDA Tech. Bull.* 926:1–20.

Hood, R. L., and C. E. Allen. 1973. Cellularity of bovine adipose tissue. *J. Lip. Res.* 14:605–610. doi:10.1016/S0022-2275(20)36840-1

Hunter, T. E., D. Suster, F. R. Dunshea, L. J. Cummins, A. R. Egan, and B. J. Leury. 2011. Dual energy X-ray absorptiometry (DXA) can be used to predict live animal and whole carcass composition of sheep. *Small Rumin. Res.* 100:143–152. doi:10.1016/j.smallrumres.2011.07.003

Kuhn, M. 2021. caret: Classification and regression training. R package version 6.0-90. Available from https://github.com/topepo/caret/

Le Cozler, Y., C. Allain, A. Caillot, J. M. Delouard, L. Delattre, T. Luginbuhl, P. Faverdin. 2019a. High precision scanning system for complete 3D cow body shape imaging and analysis of morphological traits. *Comput. Electron. Agric.* 157:447–453. doi:10.1016/j.compag.2019.01.019

Le Cozler, Y., C. Allain, C. Xavier, L. Depuille, A. Caillot, J. M. Delouard, L. Delattre, T. Luginbuhl, and P. Faverdin. 2019b. Volume and surface area of Holstein dairy cows calculated from complete 3D shapes acquired using a high precision scanning system: interest for body weight estimation. *Comput. Electron. Agric.* 165:104977. doi:10.1016/j.compag.2019.104977

Lerch, S., M. L. Lastel, C. Grandclaudon, C. Brechet, G. Rychen, and C. Feidt. 2015. In vivo prediction of goat kids body composition from the deuterium oxide dilution space determined by isotoperatio mass spectrometry. *J. Anim. Sci.* 93:4463–4472. doi:10.2527/jas.2015-9039

Lerch, S., A. D. Torre, C. Huau, M. Monziols, C. Xavier, L. Louis, Y. Le Cozler, P. Faverdin, P. Lamberton, I. Chery, et al. 2021. Estimation of dairy goat body composition: a direct calibration of eight methods. *Methods*. 186:68–78. doi:10.1016/j.ymeth.2020.06.014

Lunt, D. K., G. C. Smith, F. K. McKeith, J. W. Savell, M. E. Riewe, F. P. Horn, and S. W. Coleman. 1985. Techniques for predicting beef carcass composition. *J. Anim. Sci.* 60:1201–1207. doi:10.2527/jas1985.6051201x

López-Campos, O., J. C. Roberts, I. L. Larsen, N. Prieto, M. Juárez, M. E. R. Dugan, and J. L. Aalhus. 2018. Rapid and non-destructive determination of lean fat and bone content in beef using dual energy X-ray absorptiometry. *Meat Sci.* 146:140–146. doi:10.1016/j.meatsci.2018.07.009

Meunier, B., J. Normand, B. Albouy-Kissi, D. Micol, M. El Jabri, and M. Bonnet. 2021. An open-access computer image analysis (CIA) method to predict meat and fat content from an android smartphone-derived picture of the bovine 5th-6th rib. *Methods*. 186:79–89. doi:10.1016/j.ymeth.2020.06.023

Mevik, B.-H., R. Wehrens, and K. H. Liland. 2020. pls: Partial least squares and principal component regression. R package version 2.7-3. Available from https://CRAN.R-project.org/package=pls

Miller, G. A., J. J. Hyslop, D. Barclay, A. Edwards, W. Thompson, and C. A. Duthie. 2019. Using 3D imaging and machine learning to predict liveweight and carcass characteristics of live finishing beef cattle. *Front. Sustain. Food Syst.* 3:1–9. doi:10.3389/fsufs.2019.00030

Mitchell, A. D., M. B. Solomon, and T. S. Rumsey. 1997. Composition analysis of beef rib sections by dual-energy X-ray absorptiometry. *Meat Sci.* 47:115–124. doi:10.1016/s0309-1740(97)00045-4

R Core Team. 2020. *R: a language and environment for statistical computing*. Vienna, Austria: R Foundation for Statistical Computing. Available from https://www.R-project.org/

Realini, C. E., R. E. Williams, T. D. Pringle, and J. K. Bertrand. 2001. Gluteus medius and rump fat depths as additional live animal ultrasound measurements for predicting retail product and trimmable fat in beef carcasses. *J. Anim. Sci.* 79:137813781385. doi:10.2527/2001.7961378x

Ribeiro, F. R. B., L. O. Tedeschi, R. D. Rhoades, S. B. Smith, S. E. Martin, and S. F. Crouse. 2011. Evaluating the application of dual-X-ray absorptiometry to assess dissectible and chemical fat and

muscle from the 9th-to-11th rib section of beef cattle. *Prof. Anim. Sci*. 27:472–476. doi:10.15232/S1080-7446(15)30521-0

Robelin, J. 1981. Cellularity of bovine adipose tissues: developmental changes from 15 to 65 percent mature weight. *J. Lipid Res*. 22:452–457. doi:10.1016/S0022-2275(20)34959-2

Robelin, J., and Y. Geay. 1976. Estimation de la composition des carcasses de jeunes bovins à partir de la composition d'un morceau monocostal prélevé au niveau de la 11ème côte. II.- Composition chimique de la carcasse. *Ann. Zootech*. 25:259–272. https://hal.archives-ouvertes.fr/hal-00887588/document.

Scholz, A. M., L. Bünger, J. Kongsro, U. Baulain, and A. D. Mitchell. 2015. Non-invasive methods for the determination of body and carcass composition in livestock: dual-energy X-ray absorptiometry, computed tomography, magnetic resonance imaging and ultrasound: invited review. *Animal*. 9:1250–1264. doi:10.1017/S1751731115000336

Schröder, U. J., and R. Staufenbiel. 2006. Invited review: methods to determine body fat reserves in the dairy cow with special regard to ultrasonographic measurement of backfat thickness. *J. Dairy Sci*. 89:1–14. doi:10.3168/jds.S0022-0302(06)72064-1

Segura, J., J. L. Aalhus, N. Prieto, I. L. Larsen, M. Juárez, and O. López-Campos. 2021. Carcass and primal composition predictions using camera vision systems (CVS) and dual-energy X-ray absorptiometry (DXA) technologies on mature cows. *Foods*. 10:1118. doi:10.3390/foods10051118

Waltner, S. S., J. P. McNamara, J. K. Hillers, and D. L. Brown. 1994. Validation of indirect measures of body fat in lactating cows. *J. Dairy Sci*. 77:2570–2579. doi:10.3168/jds.S0022-0302(94)77198-8

Yan, T., C. S. Mayne, D. C. Patterson, and R. E. Agnew. 2009. Prediction of body weight and empty body composition using body size measurements in lactating dairy cows. *Livest. Sci*. 124:233–241. doi:10.1016/j.livsci.2009.02.003